

**This is a self-archived version of an original article. This version may differ from the original in pagination and typographic details.**

**Author(s):** Turkki, Paula; Laajala, Mira; Stark, Marie; Vandesande, Helena; Sallinen-Dal Maso, Heidi; Shroff, Sailee; Sävneby, Anna; Galitska, Ganna; Lindberg, A. Michael; Marjomäki, Varpu

**Title:** Slow infection due to lowering amount of intact versus empty particles is a characteristic feature of Coxsackievirus B5, dictated by the structural proteins

**Year:** 2019

**Version:** Accepted version (Final draft)

**Copyright:** © 2019 American Society for Microbiology

**Rights:** In Copyright

**Rights url:** <http://rightsstatements.org/page/InC/1.0/?language=en>

**Please cite the original version:**

Turkki, P., Laajala, M., Stark, M., Vandesande, H., Sallinen-Dal Maso, H., Shroff, S., Sävneby, A., Galitska, G., Lindberg, A. M., & Marjomäki, V. (2019). Slow infection due to lowering amount of intact versus empty particles is a characteristic feature of Coxsackievirus B5, dictated by the structural proteins. *Journal of Virology*, 93(20), e01130-19. <https://doi.org/10.1128/JVI.01130-19>

1 **Slow infection due to lowering amount of intact versus empty particles is a**  
2 **characteristic feature of Coxsackievirus B5, dictated by the structural**  
3 **proteins**

4 Paula Turkki<sup>1,2</sup>, Mira Laajala<sup>1</sup>, Marie Stark<sup>1</sup>, Helena Vandesande<sup>3</sup>, Heidi Sallinen-Dal Maso<sup>1</sup>,  
5 Sailee Shroff<sup>1</sup>, Anna Sävneby<sup>3</sup>, Ganna Galitska<sup>1</sup>, A. Michael Lindberg<sup>3</sup>, Varpu Marjomäki<sup>1</sup>

- 6 1. Department of Biological and Environmental Science Division of Cell and Molecular Biology /  
7 Nanoscience Center, University of Jyväskylä, Jyväskylä, Finland.  
8 2. Faculty of Medicine and Life Sciences, BioMediTech, Tampere University, Finland  
9 3. Department of Chemistry and Biomedical Sciences, Linnaeus University, Kalmar, Sweden

10

11

12

13

14

15

16

17

18

19

20

21

22 Corresponding author:

23

24 Varpu Marjomäki

25 Department of Biological and Environmental Science Division of Cell and Molecular Biology /  
26 Nanoscience Center, University of Jyväskylä, Jyväskylä, Finland Phone: +358 40 5634422

27 E-mail: varpu.s.marjomaki@jyu.fi

28

29 **ABSTRACT**

30 Enterovirus B species typically cause a rapid cytolysis leading to efficient release of  
31 progeny viruses. However, they are also capable of persistent infections in tissues, which  
32 are suggested to contribute to severe chronic states such as myocardial inflammation and  
33 type 1 diabetes. In order to understand the factors contributing to differential infection  
34 strategies, we constructed a chimera by combining the capsid proteins from a fast cytolysis  
35 causing echovirus 1 (EV1) with non-structural proteins from Coxsackievirus B5 (CVB5)  
36 showing persistent infection in RD cells. The results showed that the chimera behaved  
37 similar to the parental EV1 leading to efficient cytolysis in both permissive A549 and semi-  
38 permissive RD cells. In contrast to EV1 and chimera, CVB5 replicated slower in permissive  
39 cells and showed persistent infection in semi-permissive cells. However, there was no  
40 difference in the efficiency of uptake of CVB5 in A549 or RD cells in comparison to the  
41 chimera or EV1. CVB5 virus batches constantly contained significant amounts of empty  
42 capsids, also in comparison to its close relative CVB3. During successive passaging of batch  
43 containing only intact CVB5, increasing amounts of empty and decreasing amounts of  
44 infective capsids were produced. Our results demonstrate that the increased amounts of  
45 empty particles and lowering amounts of infective particles is dictated by the CVB5  
46 structural proteins leading to slowing down the infection between passages. Furthermore,  
47 the key factor for persistent infection is the low amount of infective particles produced, not  
48 the high number of empty particles accumulating.

49

50 **IMPORTANCE**

51 Enteroviruses cause several severe diseases with lytic infections that lead to rapid cell death  
52 but also persistent infections that are more silent, and lead to chronic states. Our study  
53 compared a cytolysis echovirus 1 infection to persistent coxsackievirus B5 infection by  
54 making a chimera between the structural proteins of echovirus 1 and non-structural  
55 proteins of coxsackievirus B5. Coxsackievirus B5 infection was found to lead to production of  
56 high number of empty viruses (empty capsids), that do not contain genetic material and are

57 unable to continue the infection. Coinciding with high number of empty capsids, also the  
58 amount of infective virions decreased. This characteristic property was not observed in the  
59 constructed chimeravirus, suggesting that structural proteins are in charge of these  
60 phenomena. These results shed light on the mechanisms that may cause persistent  
61 infections. Understanding events leading to efficient or inefficient infection are essential in  
62 understanding the virus caused pathologies.

63

64

65

## 66 INTRODUCTION

67 Human enteroviruses are a large group of disease causing pathogens belonging to the family  
68 of *Picornaviridae*. Enterovirus infections in man can result in different diseases, from mild  
69 flu-like diseases to more severe symptoms such as meningitis, myocarditis and paralysis.

70 The icosahedral viral capsid is formed from four capsid proteins, VP1 to VP4. VP1, VP2 and  
71 VP3 are partly exposed from the capsid while VP4 is an internal protein that becomes  
72 exposed during early entry events and A-particle formation. The single-stranded enterovirus  
73 RNA genome of positive polarity encodes for 11 proteins, seven non-structural and four  
74 structural proteins in a single open reading frame. Both 3' (ending with a poly A sequence)  
75 and 5' ends of the genome have non-translated regions which are functional in the  
76 replication process.

77 Enterovirus B species contain different serotypes and novel, only genetically characterized  
78 types, including established and well characterized serotypes Coxsackieviruses B3 (CVB3), B5  
79 (CVB5) and echovirus-1 (EV1). All CVBs use CAR as a receptor for attachment and entry (1, 2)  
80 but CVB1, 3, 5 and 6 may also use the decay accelerating factor (DAF, CD55) for attachment  
81 at the cell surface (3, 4). CAR is a tight junction localized transmembrane protein that can be  
82 used for entry into the cell (5, 6). The CVB/CAR interactions are associated with changes in  
83 the virion morphology resulting in A-particle formation and the release of the viral genome.

84 In CVB3 this phenomenon has been suggested to start already during receptor binding and  
85 virus can internalize either with or without the receptor, depending on the cell type (7-9).  
86 EV1, on the other hand, uses the collagen-binding integrin  $\alpha 2\beta 1$ , which is abundantly  
87 expressed in many cell types. EV1 internalizes together with its receptor and introduces a  
88 novel entry pathway, distinct from the natural pathway for the integrin receptors. In  
89 contrast to CVB interactions with CAR, EV1 binding to its integrin does not lead to uncoating  
90 but rather, uncoating takes place in non-acidic multivesicular structures and the viral  
91 genome is then released into the cytoplasm (10-12).

92 First signs of cell death can be seen after 4h p.i. leading to cell death within 8h p.i.  
93 depending on the virus and host cell (14). Most often the infections lead to cytolysis in cell  
94 cultures but enteroviruses may also cause persistent infections (15-19). Persistent infections  
95 have been suggested to cause chronic states leading to serious consequences, such as  
96 promoting the onset of type I diabetes in the pancreas tissue (20). Therefore, it is important  
97 to understand the detailed mechanisms behind switching between cytolytic and persistent  
98 infections. Enteroviruses have several mechanisms to cause the host cell death and,  
99 similarly, the host cell has several mechanisms to combat the virus infection and cell death  
100 (21). The interplay between host and the virus defines the outcome of the infection. Viral  
101 non-structural proteins act via inducing the host-cell shut-down, inhibiting cap-dependent  
102 translation and activating caspases. Viral structural proteins VP1, VP2 and VP3 have also  
103 been shown to have cause apoptosis, either by caspase activation or by cleavage of the  
104 poly-ADP ribose polymerase (PARP) (14).

105 In this study, a chimera between EV1 and CVB5 was constructed using reverse genetics and  
106 to study the role of non-structural and capsid proteins in the infection kinetics. The results  
107 show that the P1 region, contrary to P2 and P3, determines the efficiency and outcome of  
108 an infection. In this experimental model, the P1 region, encoding the CVB5 structural  
109 proteins, contain specific characteristics that lead to low amounts of intact virions and high  
110 incidence of empty capsids, which then slowed down the progression and kinetics of the  
111 secondary infection. We further show that the empty particles themselves did not inhibit  
112 cell binding or infection but the actual number of infective particles had a direct effect on  
113 infection kinetics.

114

115

116 **MATERIALS AND METHODS**

117 **Cells.** Virus productions and infectivity determinations were done in green monkey kidney  
118 cells (GMK) and cell experiments were carried out in human rhabdomyosarcoma (RD) and  
119 human lung carcinoma cells (A549). All cell lines were obtained from the American Type  
120 Culture Collection (ATCC) and maintained in either Eagle's Minimum Essential Medium  
121 (MEM) or Dulbecco's Modified Eagle Medium (D-MEM, Gibco Life Technologies) containing  
122 5 to 10 % of fetal bovine serum (FBS), GlutaMAX, and penicillin-streptomycin antibiotics  
123 which were obtained from Gibco, Life Technologies.

124 **Antibodies and reagents.** The following primary antibodies were used in the experiments:  
125 monoclonal anti dsRNA antibody (J2; English & Scientific Consulting Kft.), rabbit polyclonal  
126 antibody against EV1 (12), anti CVB5 (DAKO; Monoclonal Mouse, Anti-Enterovirus Clone 5-  
127 D8/1), CVB3 capsids were detected with CVA9 targeted rabbit polyclonal antibody (kind gift  
128 from Merja Roivainen, THL, Helsinki). Fluorescently conjugated goat secondary antibodies  
129 were purchased from Molecular Probes, Invitrogen.

130 **Cloning of chimera construct.** The origin of the CVB5 strain *Dalldorf* (CVB5D) and its  
131 infectious cDNA clone have been described elsewhere (22-24). This virus was used by  
132 Reagan et al. for adaptation to cytolitic infection in RD cells by massive MOI (multiplicity of  
133 infection). Normal MOI results in a persistent infection of RD cells (24). Previously a  
134 recombinant variant of the infectious cDNA clone was used to generate an ancestor for the  
135 circulating CVB5 strains in the world and as an efficient recombinant infectious cDNA clone  
136 where the P1 regions was replaced by other enterovirus B structural genes (24, 25) and  
137 upon transfection resulted in replicating chimera viruses. A plasmid, pCR Script SK+, was  
138 constructed using the infectious cDNA clone of CVB5 where the complete genome was  
139 derived from the CVB5 genome sequence and unique restriction enzyme recognition sites  
140 where introduced enabling replacement cloning of the P1 region as previously described  
141 (26). The P1 region comprised of EV 1 (Farouk strain) P1 sequence thus coding for EV1 VP1-  
142 VP4 structural proteins and the remaining part of the genome was derived from the CVB5

143 genome (EV1/CVB5cDNA aka chimera). A pSPORT plasmid was provided for positive control  
144 experiments. This cDNA clone contains a complete EV1 genome including the P1, P2, and P3  
145 sequence coding for the EV1 structural genes and corresponding NSPs (kind gift from Jeff  
146 Bergelson). The plasmids were amplified using ampicillin selection in DH5 cells and purified  
147 using Qiagen mini-prep kit. Plasmid size and correct insertion was confirmed with  
148 restriction enzyme digestion and gel electrophoresis. GMK cells were transfected with  
149 EV1cDNA and chimera using a Lipofectamine protocols, changing media after 6hr incubation  
150 at 37C. Transfected cells were passaged until GMK cells were observed to cause cytolysis.  
151 Cells were collected, freeze thawed three times cell debris was pelleted down.  
152 Supernatants were used for crude virus infection of fresh GMK cells following virus  
153 purification.

154 **Virus stock production.** After successful transfection of the plasmids and production of the  
155 crude virus extracts, GMK cells were infected with the crude virus stocks of EV1, chimera,  
156 CVB3 (*Nancy* strain from ATCC) and CVB5 for 24 h in 5-layer bottles, after which the cells  
157 were collected and lysed via three freeze-thaw cycles. Viruses were purified as described  
158 earlier (27). Sucrose gradient 5 -20% was used for CVB3 and CVB5 and fractions from 12 to  
159 21 were collected. A separate batch of CVB5 was purified using 5-20% sucrose gradient but  
160 only fractions from 14 to 21 were collected to avoid empty particles. Also, empty capsids  
161 from fractions 8-11 were collected separately. For EV1 and chimera sucrose gradient of 10-  
162 40 % were used and three fractions on basis of the A260 nm spectrophotometric data were  
163 collected. Finally, collected virus fractions were concentrated using ultracentrifugation.  
164 Virus infectivity was assessed by end-point dilution and concentration of the virus stock was  
165 determined by the measurement of absorbance at A260 nm.

166 **Cell viability assay.** Cell viability was determined with the aid of Cell Titer Glo –kit  
167 (promega). Briefly, substrate was added straight to cell media avoiding the possible loss of  
168 loosely attached cells. Two to three independent experiments with at least three replicate  
169 samples were performed in each case.

170 **Production of radioactively labelled of EV1, Chimera and CVB5.** GMK or A549 cells were  
171 cultured until sub-confluency in MEM or D-MEM supplemented with 10% FBS, 1% Glutamax  
172 and 1% penicillin/streptomycin antibiotics. Cells were infected with EV1, chimera and CVB5

173 in low methionine/cysteine medium supplemented with 1% dialyzed FBS and 1% Glutamax.  
174 The infection was allowed to proceed at + 37 °C for 3 h, after which the medium was  
175 changed into fresh low methionine/cysteine medium supplemented with 1% dialyzed FBS  
176 and 1% Glutamax containing 50  $\mu$ Ci/ml of radioactive Sulphur. The infection was allowed to  
177 proceed at + 37 °C for another 15 h or 21 h so that the total infection time was 18 h or 24 h,  
178 respectively. The cells were freeze-thawed three times, after which 100 mM Octyl  $\beta$ -D-  
179 glucopyranoside (Amresco) was added to isolate membrane bound virus particles. Cell  
180 debris was centrifuged with a microcentrifuge 5415 D (Eppendorf) at 16,000 rpm for 5 min.  
181 Supernatant was collected and added on top of 5-20% linear sucrose gradients. The  
182 gradients were collected from the top into 500  $\mu$ l fractions. An aliquot from each fraction  
183 was added with scintillation cocktail (Ultima Gold MV, Perkin Elmer) and the CPM of each  
184 fraction was measured with liquid scintillation analyzer (Tri-Carb 2910 TR, Perkin Elmer). The  
185 fraction CPM was normalized to the sum of the total CPM of the whole gradient.

186 **Immunolabeling and microscopy.** An immunolabeling experiment was carried out in cells  
187 grown on coverslips. Cells were fixed with 4% PFA for 20 min at RT. The cells were  
188 permeabilized with 0.2% Triton X-100 and then treated with primary antibodies. After  
189 primary antibody incubation the cells were washed extensively with PBS. Appropriate  
190 secondary was added to cells at RT and incubated for 30 min and finally, the cells were  
191 extensively washed with PBS and mounted with Prolong gold antifade reagent  
192 supplemented with 4',6-diamidino-2-phenylindole (DAPI) (Molecular Probes, Life  
193 Technologies). Immunolabeled samples were imaged with an Olympus IX81 microscope with  
194 a FluoView-1000 confocal setup. In total, 400 to 600 cells were imaged to manually quantify  
195 the percentage of replication and capsid positive cells.

196 **Gel electrophoresis.** The protein compositions of the virus stocks were analyzed by using a 4  
197 to 12% NuPAGE Bis-Tris gel (Novex, Life Technologies). The proteins were denatured with  
198 the gel sample buffer provided by the manufacturer (NuPAGE; Life Technologies) at 100°C  
199 before they were loaded onto the gel. The gel was stained with commassie stain including  
200 fixative.

201 **Passage assay.** A549 cells were cultured on 96-well plates close to confluency in D-MEM  
202 supplemented with 10% FBS, 1% Glutamax and 1% penicillin/streptomycin antibiotics. Cells

203 were infected with MOI 500 of EV1, chimera, CVB5 and CVB3 and the viruses were diluted in  
204 D-MEM supplemented with 1% FBS and 1% glutamax. The infection was allowed to proceed  
205 at +37 °C for 2 h, after which the medium was changed into fresh D-MEM supplemented  
206 with 10% FBS and 1% glutamax. The infection was then allowed to proceed at +37 °C for  
207 another 16 h. Next, half of the culture medium was passaged to new A549 cells and  
208 infection was allowed to proceed at +37 °C for 2 h, after which the medium was changed.  
209 The infection was then again allowed to proceed for 16 h at +37 °C. After passaging, the  
210 cells were always stained with crystal violet containing stain (8.3 mM crystal violet, 45 mM  
211 CaCl<sub>2</sub>, 10% ethanol, 18.5% formaline, and 35 mM Tris-Base) for 10 min, after which excess  
212 stain was washed with water. Finally, lysis buffer (47.5% EtOH; 35 mM sodium citrate; 12.5  
213 mM HCl) was added to dissolve the stained cells and the absorbance was measured at 570  
214 nm with a Victor X4 2030 multilabel reader (PerkinElmer).

215 **Infection in the presence of empty capsids.** A549 cells were cultured on 96-well plate in D-  
216 MEM supplemented with 10% FBS, 1% glutamax and 1% penicillin/streptomycin antibiotics.  
217 Cells were infected with the intact particles of CVB5 with MOI 0.7, 6.5, 21, 43 or 65  
218 corresponding to 0.07, 0.65, 2.1, 4.3 and 6.5 ng, respectively. The virus mixture also  
219 contained different amounts of CVB5 empty particles (1.5, 3, 6 or 9 ng). The infection was  
220 allowed to proceed in D-MEM supplemented with 1% FBS, 1% glutamax and 1%  
221 penicillin/streptomycin antibiotics at +37 °C for 20 h. Next, the cells were stained with  
222 crystal violet containing stain (8.3 mM crystal violet, 45 mM CaCl<sub>2</sub>, 10% ethanol, 18.5%  
223 formaline, and 35 mM Tris-Base) for 10 min, after which excess stain was washed with  
224 water. Finally, lysis buffer (47.5% EtOH; 35 mM sodium citrate; 12.5 mM HCl) was added to  
225 dissolve the stained cells and the absorbance was measured at 570 nm with a Victor X4  
226 2030 multilabel reader (PerkinElmer).

227 **Titration using end point dilution assay.** GMK cells were cultured on 96-well plate in MEM  
228 supplemented with 10% FBS, 1% glutamax and 1% penicillin/streptomycin antibiotics. Cells  
229 were infected with the purified viruses or supernatants derived from passage assay by  
230 preparing a dilution series in MEM supplemented with 1% FBS and 1% GlutaMAX. The  
231 infection was allowed to proceed at + 37 °C for three days, after which the cells were  
232 stained with crystal violet stain (8.3 mM crystal violet, 45 mM CaCl<sub>2</sub>, 10% ethanol, 18.5%  
233 formalin, and 35 mM Tris base). The excess stain was washed with water, and the 50%

234 tissue culture infective dose (TCID50) was calculated by comparing the number of infected  
235 and uninfected wells for eight or four replicates of the same virus concentration. The  
236 concentration at which half of the wells would be infected was extrapolated (TCID50).  
237 Finally, the TCID50 value was multiplied by 0.7 to obtain the PFU/ml value.

238 **RT-qPCR.** A549 or RD cells were infected with EV1, chimera or CVB5 with MOI 10 in D-MEM  
239 supplemented with 1% FBS and 1% glutamax. After 1 h, cells were washed with PBS, after  
240 which the infection was allowed to proceed in D-MEM supplemented with 1% FBS and 1%  
241 glutamax for 2, 8, 24 or 48 h. At the end, the cells were freeze-thawed three times and cell  
242 debris was pelleted down at full speed with table top centrifuge. Viral RNA from the  
243 supernatant was extracted according to the instructions of the manufacturer using QiAmp  
244 viral RNA Mini Kit (Qiagen). Reverse transcription was carried out for positive strand RNA  
245 using 1.2  $\mu$ M antisense (5'-GAAACACGGACACCCAAAGTA) primer, 20 U M-MLV reverse  
246 transcriptase (Promega), 4 U RNAsin ribonuclease inhibitor (Promega) and dNTPs  
247 (Promega). The generated cDNA copy of the RNA was applied to qRT – PCR amplification  
248 using the 7500 Real-Time PCR System (Applied Biosystems) with 7500 SDS analysis software.  
249 Each reaction contained 5  $\mu$ l template, 1 X Power SYBR Green Master Mix (Applied  
250 Biosystems) and 0.75  $\mu$ M of antisense (5'-GAAACACGGACACCCAAAGTA) and sense (5'-  
251 CGGCCCTGAATGCGGCTAA) primers for a final volume of 20  $\mu$ l. The thermocycling protocol  
252 was executed as follows: pre – amplification step (involving denaturation and DNA  
253 polymerase activation) at 95 °C for 10 min.; 10 cycles of 15 s. at 95 °C, 30 s. at 64 °C – 55 °C  
254 (following a touch – down of 1 °C per cycle), and 40 s. at 72 °C; 30 cycles of 15 s. at 95 °C, 30  
255 s. at 55 °C, and 40 s. at 72 °C; and dissociation curve generation for 1 cycle of 15 s. at 95 °C, 1  
256 min. at 60 °C, and 15 s. at 95 °C. Each reaction was run in triplicate.

257

258

259

260

261 **RESULTS**262 **Enterovirus chimera containing the structural proteins of EV1 and non-structural proteins**  
263 **of CVB5 leads to an efficient replication and cytolysis in GMK and A549 cells, with**  
264 **infection kinetics resembling EV1**

265 By using a previously described backbone of the CVB5 genome infectious cDNA clone (Fig  
266 1A), replicating CVB5 and EV1/CVB5 viruses were generated. In addition, EV1 viruses were  
267 generated by transfection of an infectious cDNA clone in GMK cells. EV1, CVB5 and the  
268 chimera viruses infected GMK cells with a rather similar kinetics and cytolysis was typically  
269 seen after first 24 h of infection. EV1 and chimera both lead to efficient production of  
270 progeny viruses showing high infectivity and high protein concentration of 440 µg/ml and  
271 870 µg/ml, respectively (Fig. 1B). CVB5 preparations had almost two logs lower measured  
272 virus titers but, in contrast, a significantly higher protein amount in comparison to the  
273 produced virus titers (pfu) (Fig 1B). Next, SDS-PAGE analysis of purified virus stocks was  
274 conducted in order to verify the purity of the viruses (Fig 1C). Similar protein amounts of all  
275 the virus stocks showed two clear bands corresponding to sizes between 25-37 kDa of  
276 approximately the same amount, indicating that all stocks were pure from major protein  
277 contaminants and contained only the viral capsid proteins.

278 Virus infectivity and infection kinetics were then studied in more detail in both permissive  
279 A549 and semi-permissive RD cell lines. A549 cells contain abundant amounts of the virus  
280 receptors CAR, DAF and  $\alpha 2\beta 1$  integrins on their cell surface indicating these cells should be  
281 permissive for all three viruses. RD cells on the other hand have been reported to have none  
282 or very limited CAR expression with only subpopulations of cells expressing the CAR on their  
283 cell surface (28).

284 First, A549 cells were infected with equal protein amounts of virus stocks and cell viability  
285 was measured at 12h and 24 h p.i. (Fig 1D). EV1 and chimera lead to rapid cytolysis: by 12h  
286 p.i. only half of the cells were alive and at 24 h p.i. the complete cytolysis was observed.  
287 Cytolytic capacity of CVB5 was notably slower, with 70 % of cells still viable at 24 h p.i.  
288 showing that cell destruction was greatly delayed. However, at 72 h (data not shown), also  
289 CVB5 demonstrated complete cytolytic efficiency. We then set out to compare cell viability  
290 after using similar number (virus titers) of infective particles (Fig 1E). The results showed a

291 similar trend as seen with infections with equal protein amounts, suggesting that CVB5  
292 infection kinetics was delayed when compared to EV1 and chimera at 24 h p.i.

293 Since CVB5 is known to cause persistent infection in RD cells, our next aim was to  
294 characterize the chimera infection in these cells as well. RD cells were infected first with  
295 equal protein amounts of virus stocks and cell viability was determined at 12 h and 24 h p.i.  
296 The results showed that EV1 and chimera were as cytolytic in RD cells as in A549 cells;  
297 around half of the cells had died at 12h p.i. and almost entire cultures had been destroyed  
298 at 24 h p.i. (Fig 1F). On the contrary, at 24h, only one third of CVB5 infected cells had lysed  
299 and even when the infection was continued until 48 h p.i., cell viability remained the same  
300 (data not shown). Again, we performed another viability assay using the same number of  
301 infective particles (Fig 1G). This experiment showed that not even high amounts of infective  
302 virions were able to cause lytic CVB5 infection in RD cells. At 12 h there was slight decrease  
303 in cell viability, but at 24 h CVB5 treated RD cells were as viable as the control. In contrast,  
304 EV1 and chimera showed efficient cytolytic infection.

305 Altogether, the results suggested that the chimera, consisting of EV1 capsid proteins and  
306 CVB5 non-structural proteins, was highly infective and cytolytic in both A549 and RD cells, in  
307 contrast to CVB5, suggesting that the structural proteins are contributing to the switch to  
308 cytolytic infection.

309

310 **CVB3 and CVB5 both show persistent carrier culture infection in RD cells whereas in**  
311 **permissive A549 cells CVB5 has significantly slower infection kinetics**

312 In order to study the possible role of the entry receptor, we included CVB3 in our studies as  
313 previous studies has shown that both CVB3 and CVB5 use CAR and DAF. First, we monitored  
314 CVB3 and CVB5 infection in both A549 and RD cells. We monitored viability of cells that  
315 were infected with equal MOI of viruses until 96 h p.i.. In A549 cells both viruses lead to the  
316 destruction of the entire cell culture within 96 h confirming a lytic replication mode in  
317 permissive cells (Fig 2A). Although both viruses demonstrated cytolytic replication of the  
318 cells in the end, CVB5 was notably slower than CVB3. At 24 h p.i., almost all of the CVB3  
319 infected cells had died, while around 60 % of the CVB5 infected cells were still viable.

320 Infected RD cell cultures did not show apparent cell lysis with either of the viruses. Confocal  
321 microscopy confirmed the presence of viral capsid protein in minority of the cells in the  
322 culture during the 96 h time series (data not shown), suggesting that both viruses caused  
323 persistent infection in these cells. Even after 9 days of incubation with the viruses, no  
324 significant cytotoxicity was observed for the cell culture (data not shown). Since CVB5  
325 infection was notably slower in A549 when compared to CVB3 when using the same MOI,  
326 similar to what was observed with EV1 and chimera (Fig 1B), we next studied in more detail  
327 the kinetics of capsid and dsRNA production. We infected A549 and RD cells with equal MOI,  
328 fixed the cells at different timepoints, immunolabelled against dsRNA and virus capsids and  
329 imaged with confocal microscopy. After imaging, we quantified the images in order to  
330 determine the presence of capsid positive cells (Fig 2B and D). In A549 cells, there was a  
331 clear difference in the percentage of dsRNA positive cells when CVB3 and CVB5 infections  
332 were compared. At 6 h p.i, about 35 % of infected cells showed positive label for dsRNA  
333 during CVB3 infections, whereas only 10% of CVB5 infected cells were positive at same  
334 timepoint. However, at 12h both infections were showing equal amount of dsRNA positive  
335 cells. As the same experiment was performed with RD cells (Fig 3D), there was no major  
336 difference in the number of cells showing infection between the two viruses for the first 48  
337 h; viruses could only replicate in a small subpopulation of cells. Cells infected with either of  
338 the virus showed only around 10 % of the population that had newly synthesized capsid  
339 proteins present until 48 h p.i.

340 To conclude, these results suggested that both, CVB3 and CVB5, eventually lead to cytolytic  
341 infection in A549 cells and persistent infection of the RD cells but, importantly, CVB5  
342 infection kinetics is slower than CVB3.

343

344

#### 345 **CVB5 batches produced in GMK cells contain high-amounts of empty capsids**

346 As CVB5 was notably slower in A549 cells, we started to compare the CVB3 and CVB5 virus  
347 stocks in detail. First, as we compared the pfu/ml to mg/ml status of CVB3 and CVB5, we  
348 noticed a similar phenomenon as when compared to EV1 and Chimera (Fig 1B): CVB5

349 contained more protein in relation to its pfu/ml when compared to CVB3 (Fig 3A). For more  
350 detailed understanding of the status of the viruses in purified batches, we performed  
351 transmission electron microscopy (TEM) analysis of the virus stocks (Fig 3B). Negatively  
352 stained TEM samples showed that EV1 and chimera mostly contained infectious virions (N-  
353 form), intact particles showing as light-coloured particles in TEM images. Only a small  
354 percentage of empty, dark labeled particles were observed per frame. In contrast, CVB5  
355 batches had approximately 40 % of the virus particles with dark interior, suggesting that the  
356 batch contained significant portion of empty capsids. This was an interesting finding and  
357 possibly an explanation for differences observed during infection between these viruses.

358 Furthermore, when purified batches of CVB3 and CVB5 were compared, TEM analysis  
359 showed that CVB5 batch consisted of only approximately 50 % intact particles, whereas  
360 CVB3 batch contained mostly intact particles (Fig 3B, bottom row). Altogether, these results  
361 showed that CVB5 batches systematically contained high proportions of empty particles  
362 further explaining high virus protein concentration vs infectivity readings.

363

#### 364 **Purified batch of CVB5 containing only intact particles leads to efficient infection**

365 We then continued to further elucidate the role of the empty particles with CVB5 that only  
366 contained complete virions, N particles. The intact viruses (160 S form of the virus) were  
367 separated from the empty virions and isolated from the bottom part of the 5-20% sucrose  
368 gradient. TEM analysis using negative staining confirmed that the new virus batch contained  
369 only intact virions (Fig 4A). Gradient fractionation of metabolically labeled viruses revealed  
370 no major differences between the various viruses in GMK cells and suggested that all of  
371 them contained a majority of N particles and a rather similar low amount of empty virions  
372 (Fig 4B). Similar results were obtained with A549 cells (Fig 4B). Also, cell viability  
373 measurement in A549 and RD cells after infection for 24 h, with the same amount of intact  
374 virus, showed that CVB5 infection was almost as efficient in infection in comparison to EV1,  
375 chimera and CVB3 in A549 cells and non-cytolytic in RD cells (Fig 4C). In order to look at the  
376 replication kinetics in more detail, we decided to compare the amount of replication using  
377 qPCR of the (+) strand RNA after using similar amount of infective particles from different  
378 constructs in A549 cells. The results showed that the amount of virus load taken up during 2

379 h is very similar between EV1 and chimera (Fig. 4D). Interestingly the, amount of CVB5 taken  
380 up during 2 h was even higher. There was no difference between the amounts of RNA  
381 produced after 8, 24 or 48 h. This result was replicated in an immunolabelling analysis  
382 detecting the replication intermediate dsRNA and capsid by confocal microscopy (Fig 4E):  
383 EV1, chimera and CVB5 (intact) showed ample amount of dsRNA and capsid in A549 cells.

384 qPCR evaluation of CVB5 replication in RD cells showed also that the uptake during 2 h to RD  
385 cells was as efficient as with other constructs (Fig 4D). However, there was a clear difference  
386 after 8 h in the amount of RNA produced: the amount of RNA was significantly lower, and  
387 the lower amounts were also evident after 24 and 48 hours.

388

389 **Generation of empty capsids during CVB5 replication is a characteristic trait that shows up**  
390 **during serial passaging but do not explain the silencing of the infection**

391 We then wanted to see how the infection would proceed within next generations when  
392 using the CVB5 batch that only had intact particles. A549 cells were infected with equal  
393 MOI and the infection efficiency as CPE was monitored during several passages until passage  
394 4 (Fig 5A). Crystal violet staining of the passaged plates revealed that the first overnight  
395 infection by all viruses readily lifted the cells from the wells indicative of good infection.  
396 However, when we dissolved the crystal violet color and quantified the signal, the results  
397 showed that already during this first CPE, CVB5 showed lower amount of detached cells in  
398 comparison to other viruses. The next passages showed a much clearer difference between  
399 CVB5 and other viruses, suggesting that almost all cells survived the CVB5 infection. In  
400 contrast, there was no significant difference between EV1, chimera and CVB3, all of them  
401 showing high CPE in all passages.

402 As the lower CPE for CVB5 could result either from higher number of empty or lower  
403 number of infective particles, we measured the amounts of infectious virus particles  
404 produced in each step from different constructs. The results showed that the EV1, chimera  
405 and CVB3 all had high amounts of viruses in all passages although the actual pfu/ml varied in  
406 between  $10^6$  and  $10^7$  particles (Fig 6B). Strikingly, quantification of the virions from CVB5  
407 showed low pfu/ml of only  $10^5$  in the first passage, and from there on the titers were too

408 low to determine titer measurements. The titers for CVB5 kept under detection level during  
409 all consecutive passages suggesting that the infectivity dropped very soon to a low level.

410 In order to study if the presence of empty particles could affect the CPE in A549 cells, we  
411 performed two different experiments: 1) First we used a similar amount of intact CVB5  
412 particles, on top of which we added increasing amounts of empty particles. This approach  
413 showed that the increasing amounts of empty capsids, the highest exceeding the number of  
414 intact virions by about 1.4 fold, did not affect the infectivity of CVB5. 2) Next, we used  
415 increasing amounts of intact CVB5 virions on top of which we added a similar and high  
416 amount of empty particles (Fig. 5C). Also this approach revealed only minor changes in cell  
417 viability, suggesting that at least the amounts of empty virions used in the assay did not  
418 harm CVB5 infection efficiency.

419 Altogether, these results show that CVB5 batches have a tendency to produce lower  
420 amount of intact particles and increased amounts of empty virus particles. The presence of  
421 empty capsids does not affect infectivity, whereas the lowering amount of infective particles  
422 lead to slower infection kinetics of permissive A549 cells.

423

424

425

## 426 **DISCUSSION**

427 Chimeric enteroviruses as an experimental approach has been an informative tool in  
428 studying different enteroviral traits. Recently, a chimeric CVB3 strain with 5' NTR of  
429 poliovirus was found to lead to less efficient replication than the parental strain. This was  
430 found to promote immunity against CVB3-mediated heart and pancreatic diseases,  
431 suggesting that chimeric viruses are useful in vaccine research (29). Another study with  
432 chimeric constructs between respiratory (EV-D68) and an enteric (EV-D94) EV, suggested  
433 that tropism was dictated by the capsid proteins, while innate immunity was transferred via  
434 the NS-proteins, providing information on the roles of capsid and NS-proteins (30). In  
435 general, the enterovirus type is determined by its P1 region. Due to high extent of sequence  
436 conservation in the P2 and P3 regions, this part of the genome may be regarded as a

437 supportive and replicative backbone to the type determining P1 region. Recombination  
438 takes place in the nature and e.g. different chimeric variants between endogenous viruses  
439 and vaccine strains appear time to time (31). Also, our results showed that viral structural  
440 elements between members of the enterovirus B species are easily interchangeable within  
441 the EV-B group.

442 Our goal here was to see if chimeric enterovirus could reveal new information regarding the  
443 mechanisms of persistent infections and the efficiency of lytic replication. We constructed a  
444 chimera consisting of EV1 structural proteins and CVB5 non-structural proteins. These  
445 parental viruses were selected for their known differences in their infection kinetics in cell  
446 culture. EV1 is a fast-acting cytolitic virus, whereas CVB5 has been shown to lead to slower  
447 infection, when using the CVB5 strain and the cell types studied. The results altogether  
448 showed that the chimera was functional, leading to fast cytolysis in A549 cells, highly  
449 resembling the EV1 infection kinetics. In contrast, CVB5 led to significantly slower onset of  
450 replication and CPE in A549 cells.

451 In cell cultures, enteroviruses usually cause lytic infections resulting in cell death from 6 h  
452 p.i. onwards. One exception to this rule seem to be the human rhabdomyosarcoma cell line  
453 (RD), which has been shown to result in persistent infection when infected with CVB20 (32),  
454 CVB3 (28) and CVB5 (16), whereas in Hela and A549 cells, these viruses cause cytolitic  
455 infection (data not shown). One hypothesis for this phenomenon has been low or negligible  
456 transient expression of CAR in RD cells (28). It is believed that the low CAR expression helps  
457 the virus to sustain a carrier culture persistency in RD cell cultures as only subpopulation of  
458 the cells can get infected. Our data here supports this hypothesis, as only subpopulation of  
459 the cells got infected and clear signs of cytotoxicity and cytolysis was observed in those  
460 infected cells (data not shown), but the cell culture in general kept viable. In addition to  
461 persistent infections, it seems that enteroviruses cultured in RD cells obtain adaptations  
462 that lead to increased CPE within the culture, and eventually to total cytolysis of the culture  
463 (26, 33). After nine passages of CVB2 Ohio-strain (CVB20) in RD cells Polacek et al (32)  
464 reported a phenotype of CVB20 that caused cytolysis of the culture. Both the parental and  
465 the adapted strains lead to similar titers of cytolitic viruses in Hela cells, while parental  
466 strain was showing decreased replication level in RD cells. Cytolytic trait was identified to be  
467 due to single amino acid change within the exposed region of VP1 capsid protein (26),

468 suggesting a role in receptor usage. By using a high MOI, it was however possible to adapt  
469 the persistent CVB2O infection to a cytolytic one and the single mutation needed was a  
470 single mutation in VP1 (26). CVB3 has also been previously shown to adapt to RD cells by  
471 serial passaging causing increased CPE in these cells. The obtained CVB3-RD strain had  
472 increased affinity to bind DAF in comparison to the prototype strain CVB3-Nancy (23). This  
473 ability has been later mapped to two amino acid changes in the VP2 capsid protein (34).  
474 Although both DAF and CAR mediate tight binding of the CVB3-RD particle, only CAR  
475 supports the A-particle formation and internalization of the virus, while DAF most likely has  
476 a sequestering role on the cell surface (35). In addition to receptor usage, even closely  
477 related viruses can promote differential antiviral effects in their host cell. For example, two  
478 viruses that are known to cause hand-foot-and-mouth disease (HFMD), EV71 and CVA16,  
479 lead to differential activation of the interferon response in RD cells, further reflecting to  
480 their infection efficiency (36).

481 Our studies on EV1, chimera and CVB5, demonstrated that chimera had similar  
482 characteristics to EV1 with respect to virus infection kinetics. Chimera showed efficient  
483 production of infective virus particles, efficient replication as judged by qPCR and cytolysis  
484 with a similar time scale as with parental EV1. As CVB5 showed negligible cytolysis in RD  
485 cells, the results demonstrate that the 5'UTR or the non-structural P2-P3 part of the  
486 genome does not dictate the differences between the chimera/EV1 and CVB5. Altogether  
487 these results suggested that the differences between CVB5 and EV1/chimera rely on the  
488 structural proteins comprising the viral capsid. This led us to consider if receptor binding and  
489 entry pathway could explain the marked difference between the constructs. In order to  
490 compare CVB5 to another CVB with abilities to bind to same receptors, CAR and DAF, we  
491 chose to use CVB3 in our experiments. Despite these similarities, there was still a clear  
492 difference between these viruses, CVB3 being more cytolytic and efficient than CVB5 in  
493 permissive A549 cells, suggesting that other factors than actual receptor binding would  
494 contribute to the slower lysing of the cells during CVB5 infection. Furthermore, qPCR  
495 analysis of the uptake efficiency showed no difference between the viruses. We therefore  
496 started to look for other differences between these viruses.

497 The high number of empty virions in the CVB5 virus batches seemed to be the most  
498 apparent difference between the two CVBVs. This was proven by TEM and by careful

499 characterization of protein and infective particle content of the preparations. Strikingly, the  
500 infection efficiency of the CVB5 batch containing only intact and infective full viruses did not  
501 differ much between the viruses during the first round of infection. The presence of empty  
502 capsid thus seemed to be a likely explanation to the reduced efficiency of infection in  
503 subsequent passages. However, detailed analysis of the role of empty viruses, by adding  
504 various amounts of empty viruses on top of intact virions showed clearly that the  
505 accumulation of empty virions does not interfere with infection using the applied  
506 experimental set up. The results thus indicated that low amounts of intact viruses produced  
507 and not the high amounts of empty viruses is the determining factor for the slowing down  
508 of infection. Why does this then occur? If we start with fully infective particles, the amount  
509 of infective particles drops in comparison to chimera and EV1 already after the first passage  
510 and is under the detection limit already during the second passage.

511 Empty capsids are typically produced in varying amounts among picornavirus infections.  
512 They sediment around 70 to 80 S in sucrose gradients and contain VP0, VP1 and VP3 (37-  
513 41), although there are reports of FMDV empty capsids that contain also mature VP2 and  
514 VP4 (42). One explanation for these procapsids is that they form a reservoir of capsids  
515 where the genome may possibly be inserted (38, 40). Despite empty capsids being common,  
516 there are also families of picornaviruses, such as human parechoviruses and especially  
517 Ljungan virus, that have not been reported to produce empty particles (43). Ljungan virus  
518 shows substantial differences in the capsid structure indicating that a different capsid form  
519 could have an effect on the genome encapsidation and thus play a role in the production of  
520 empty particles (43).

521 There is some literature about the presence of defective infective particles (DIP) that  
522 naturally interfere infection and replication of many viruses, including hepatitis B and C,  
523 influenza A virus, Dengue virus, and poliovirus (44-47). DIPs show deletions of one or  
524 multiple genes and thus cannot replicate alone, but during co-infection with fully infective  
525 viruses, will interfere with the outcome of the virus infection (45). In our experiments, the  
526 TEM analysis and the metabolic labeling of CVB5 showed that our batches contained truly  
527 empty capsids without RNA content. Also, the fact that increasing amounts of CVB5 empty  
528 viruses did not interfere with intact virions, argue against DIPS present in our CVB5  
529 population.

530 One possible reason for the observed low production of infective particles with CVB5 is to  
531 interfere with the virus assembly step in the cytoplasm. How could that be affected by the  
532 structural proteins, however, remains a puzzle. Could the assembly of new virions be  
533 disturbed during CVB5 infection? Altogether, our data here shows that capsid proteins are  
534 determining the efficiency of infection for the studied constructs, whereas 5'UTR and the  
535 non-structural proteins did not determine the switch between cytolytic and more silent  
536 infection in A549 and RD cells, respectively. CVB5 infection leads to production of lower  
537 amounts of infective virions in relation to high amount of empty virus particles, which delays  
538 the infection progress. If the empty capsids are removed, CVB5 infection will lead to more  
539 efficient CPE but will soon start getting slower again, suggesting that the production of  
540 empty particles in the expense of infective virions is a characteristic property of this CVB5  
541 strain in these type of cells, a feature previously reported for several different  
542 enteroviruses. Furthermore, CVB5 behavior was different from CVB3, which uses the same  
543 cell surface receptors, further demonstrating that the slowing down may be more linked to  
544 affecting assembly rather than viral entry.

#### 545 **FIGURE LEGENDS**

546 **FIG 1. Production and characterization of EV1, chimera and CVB5 stocks in GMK cells.** A) Schematic  
547 illustration of the chimera containing the P1 region from EV1 and P2 and P3, including the 5'UTR from CVB5.  
548 B) Graph showing the infectivity (pfu/ml) and protein concentration of the produced virus stocks. C) SDS-PAGE  
549 analysis of virus stocks. Each lane has 1 µg of virus. Graphs showing the cell viability of infected A549 cells (D  
550 and E) and RD cells (F and G) detected at 12h and 24h p.i.. In D and F, infections were done with equal protein  
551 concentration of 0,7 µg/ml, corresponding to MOI 500 of EV1 and chimera and MOI 9 of CVB5. In E and G,  
552 infections were done with MOI 500.

553

554 **FIG 2. Characterization of CVB3 and CVB5 infection in A549 and RD cells.** A) Cell viability measurements  
555 during different timepoints in A) A549 cells. B) Quantification showing the percentage of cells positive for  
556 capsid and dsRNA labelling in A549 cells. C) cell viability in RD cells D) IF labeling quantifications in RD cells. Cell  
557 viability assay Infections were done with MOI 65, with corresponding protein concentrations of 0,01 µg/ml for  
558 CVB3 and 1 µg/ml for CVB5. IF labeling quantifications were made from three independent experiments with  
559 three replicates in each of them (total of 750 to 1350 cells / sample). Infections were done with MOI 65, with  
560 corresponding protein concentrations of 0,01 µg/ml for CVB3 and 1 µg/ml for CVB5. Results are averages from  
561 four samples within one representative experiment with SEM. Statistical significances are marked with \*\* <  
562 0,01, \*\*\* < 0,001, \*\*\*\* < 0,0001.

563 **FIG 3. CVB5 produced empty virus capsids in GMK cells.** A) Graph showing the infectivity (pfu/ml) and protein  
564 concentration of the CVB3 and CVB5 virus stocks produced in GMK cells. B) Structural characterization of the  
565 virus stocks with the aid of TEM images and negative staining with representative magnifications. Scale bar  
566 200 nm.

567

568 **FIG 4. CVB5 infection kinetics with batch containing only intact viruses** A) TEM image of negative stained  
569 differentially produced CVB5 batch that mostly contained intact virus particles. B) Graph showing the cpm  
570 counts (% of total cpm) after virus infections of GMK or A549 cells performed in the presence of radioactive  
571 methionine/cysteine. Cells were infected with MOI 25. C) A549 or RD cells were infected with MOI 500 of EV1,  
572 chimera, CVB5 or CVB3 and cell viability (ATP) was determined at 24 h p.i.. D) RT-qPCR from EV1, chimera and  
573 CVB5 infected A549 and RD cells. The cells were infected with MOI 10, and after 1 h the medium was changed.  
574 The amount of positive sense RNA was determined from the lysed cells at 2,8,24 and 48 h p.i. cDNA of chimera  
575 was used as a positive control. E) Confocal images showing dsRNA and capsid distribution from A549 cells that  
576 were infected with EV1, chimera or CVB5, fixed and immunolabelled. 500 PFU/cell was first bound on ice for 1  
577 h, after which excess virus was washed with 0.5% BSA in PBS. Infection was then allowed to proceed at +37 °C  
578 for 6 h.

579

580 **FIG 5. The infection efficiency of CVB5 is decreased in next generations which is not due to disturbance of**  
581 **empty particles.** A) Passage assay with CVB5 batch containing only intact particles at start. A549 cells were  
582 infected with EV1, Chimera, CVB5 and CVB3 and CPE was monitored for four generations by passaging a similar  
583 amount of culture supernatant to the next wells at 18 h intervals. Initial infection was done with MOI 500 for  
584 all constructs and the medium was changed after 2 h. B) PFU/ml values of supernatants from the passage  
585 assay in A, were determined with end-point dilution assay. C) CPE assay with intact CVB5 particles was carried  
586 out in the presence of increasing amount of CVB5 empty particles or increasing amount of intact particles (MOI  
587 43 (4.3 ng), MOI 21 (2.1 ng), MOI 6.5 (0.65 ng), MOI 0.7 (0.07 ng)). Intact and empty particles were mixed  
588 together and added on A549 cells. The infection was allowed to proceed for 20 h, after which the cell viability  
589 was determined by crystal violet staining.

590

591

## 592 REFERENCES

- 593 1. Bergelson, J. M., J. A. Cunningham, G. Droguett, E. A. Kurt-Jones, A. Krithivas, J. S. Hong,  
594 M. S. Horwitz, R. L. Crowell, and R. W. Finberg. 1997. Isolation of a common receptor for  
595 Coxsackie B viruses and adenoviruses 2 and 5. *Science*. **275**:1320-1323.
- 596 2. Martino, T. A., M. Petric, H. Weingartl, J. M. Bergelson, M. A. Opavsky, C. D. Richardson,  
597 J. F. Modlin, R. W. Finberg, K. C. Kain, N. Willis, C. J. Gauntt, and P. P. Liu. 2000. The  
598 coxsackie-adenovirus receptor (CAR) is used by reference strains and clinical isolates  
599 representing all six serotypes of coxsackievirus group B and by swine vesicular disease virus.  
600 *Virology*. **271**:99-108. doi: 10.1006/viro.2000.0324 [doi].
- 601 3. Bergelson, J. M., J. G. Mohanty, R. L. Crowell, N. F. St John, D. M. Lublin, and R. W.  
602 Finberg. 1995. Coxsackievirus B3 adapted to growth in RD cells binds to decay-accelerating  
603 factor (CD55). *J. Virol.* **69**:1903-1906.

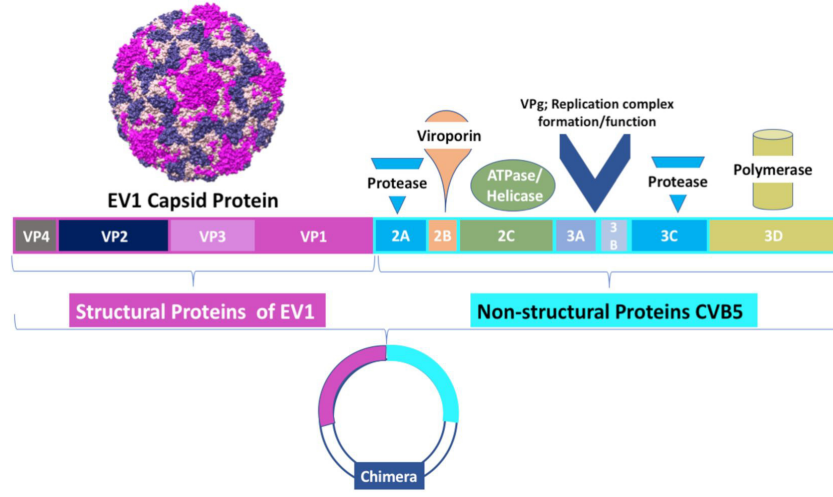
- 604 4. **Shafren, D. R., R. C. Bates, M. V. Agrez, R. L. Herd, G. F. Burns, and R. D. Barry.** 1995.  
605 Cocksackieviruses B1, B3, and B5 use decay accelerating factor as a receptor for cell  
606 attachment. *J. Virol.* **69**:3873-3877.
- 607 5. **Bergelson, J. M., J. F. Modlin, W. Wieland-Alter, J. A. Cunningham, R. L. Crowell, and R.**  
608 **W. Finberg.** 1997. Clinical coxsackievirus B isolates differ from laboratory strains in their  
609 interaction with two cell surface receptors. *J. Infect. Dis.* **175**:697-700.
- 610 6. **Cohen, C. J., J. T. Shieh, R. J. Pickles, T. Okegawa, J. T. Hsieh, and J. M. Bergelson.** 2001.  
611 The coxsackievirus and adenovirus receptor is a transmembrane component of the tight  
612 junction. *Proc. Natl. Acad. Sci. U. S. A.* **98**:15191-15196. doi: 10.1073/pnas.261452898 [doi].
- 613 7. **Coyne, C. B., and J. M. Bergelson.** 2005. CAR: a virus receptor within the tight junction.  
614 *Adv. Drug Deliv. Rev.* **57**:869-882. doi: S0169-409X(05)00016-5 [pii].
- 615 8. **Coyne, C. B., L. Shen, J. R. Turner, and J. M. Bergelson.** 2007. Cocksackievirus entry across  
616 epithelial tight junctions requires occludin and the small GTPases Rab34 and Rab5. *Cell. Host*  
617 *Microbe.* **2**:181-192. doi: S1931-3128(07)00163-1 [pii].
- 618 9. **Delorme-Axford, E., Y. Sadovsky, and C. B. Coyne.** 2013. Lipid raft- and SRC family kinase-  
619 dependent entry of coxsackievirus B into human placental trophoblasts. *J. Virol.* **87**:8569-  
620 8581. doi: 10.1128/JVI.00708-13 [doi].
- 621 10. **Karjalainen, M., N. Rintanen, M. Lehtonen, K. Kallio, A. Maki, K. Hellstrom, V.**  
622 **Siljamaki, P. Upla, and V. Marjomaki.** 2011. Echovirus 1 infection depends on biogenesis of  
623 novel multivesicular bodies. *Cell. Microbiol.* **13**:1975-1995. doi: 10.1111/j.1462-  
624 5822.2011.01685.x; 10.1111/j.1462-5822.2011.01685.x.
- 625 11. **Rintanen, N., M. Karjalainen, J. Alanko, L. Paavolainen, A. Maki, L. Nissinen, M.**  
626 **Lehtonen, K. Kallio, R. H. Cheng, P. Upla, J. Ivaska, and V. Marjomaki.** 2012. Calpains  
627 promote alpha2beta1 integrin turnover in nonrecycling integrin pathway. *Mol. Biol. Cell.*  
628 **23**:448-463. doi: 10.1091/mbc.E11-06-0548.
- 629 12. **Marjomaki, V., V. Pietiainen, H. Matilainen, P. Upla, J. Ivaska, L. Nissinen, H.**  
630 **Reunanen, P. Huttunen, T. Hyypia, and J. Heino.** 2002. Internalization of echovirus 1 in  
631 caveolae. *J. Virol.* **76**:1856-1865.
- 632 13. **Marjomaki, V., P. Turkki, and M. Huttunen.** 2015. Infectious Entry Pathway of  
633 Enterovirus B Species. *Viruses.* **7**:6387-6399. doi: 10.3390/v7122945 [doi].
- 634 14. **Buenz EJ, and Howe CL.** 2006. Picornaviruses and cell death. *Trends in Microbiology.*  
635 **14**:28-36. doi: <https://doi.org/10.1016/j.tim.2005.11.003>.
- 636 15. **Chehadeh, W., J. Kerr-Conte, F. Pattou, G. Alm, J. Lefebvre, P. Wattre, and D. Hober.**  
637 2000. Persistent infection of human pancreatic islets by coxsackievirus B is associated with  
638 alpha interferon synthesis in beta cells. *J. Virol.* **74**:10153-10164.

- 639 16. **Argo, E., B. Gimenez, and P. Cash.** 1992. Non-cytopathic infection of  
640 rhabdomyosarcoma cells by coxsackie B5 virus. *Arch. Virol.* **126**:215-229.
- 641 17. **Alidjinou, E. K., F. Sane, A. Bertin, D. Caloone, and D. Hober.** 2015. Persistent infection  
642 of human pancreatic cells with Coxsackievirus B4 is cured by fluoxetine. *Antiviral Res.*  
643 **116**:51-54. doi: 10.1016/j.antiviral.2015.01.010 [doi].
- 644 18. **Engelmann, I., E. K. Alidjinou, A. Bertin, J. Bossu, C. Villenet, M. Figeac, F. Sane, and D.**  
645 **Hober.** 2017. Persistent coxsackievirus B4 infection induces microRNA dysregulation in  
646 human pancreatic cells. *Cell Mol. Life Sci.* . doi: 10.1007/s00018-017-2567-0 [doi].
- 647 19. **Kim, K. S., S. Tracy, W. Tapprich, J. Bailey, C. K. Lee, K. Kim, W. H. Barry, and N. M.**  
648 **Chapman.** 2005. 5'-Terminal deletions occur in coxsackievirus B3 during replication in  
649 murine hearts and cardiac myocyte cultures and correlate with encapsidation of negative-  
650 strand viral RNA. *J. Virol.* **79**:7024-7041. doi: 79/11/7024 [pii].
- 651 20. **Hyoty, H.** 2016. Viruses in type 1 diabetes. *Pediatr. Diabetes.* **17 Suppl 22**:56-64. doi:  
652 10.1111/pedi.12370 [doi].
- 653 21. **Harris, K. G., and C. B. Coyne.** 2014. Death waits for no man--does it wait for a virus?  
654 How enteroviruses induce and control cell death. *Cytokine Growth Factor Rev.* **25**:587-596.  
655 doi: 10.1016/j.cytogfr.2014.08.002 [doi].
- 656 22. **CROWELL, R. L., and J. T. SYVERTON.** 1961. The mammalian cell-virus relationship. VI.  
657 Sustained infection of HeLa cells by Coxsackie B3 virus and effect on superinfection. *J. Exp.*  
658 *Med.* **113**:419-435.
- 659 23. **Reagan, K. J., B. Goldberg, and R. L. Crowell.** 1984. Altered receptor specificity of  
660 coxsackievirus B3 after growth in rhabdomyosarcoma cells. *J. Virol.* **49**:635-640.
- 661 24. **Gullberg, M., C. Tolf, N. Jonsson, M. N. Mulders, C. Savolainen-Kopra, T. Hovi, M. Van**  
662 **Ranst, P. Lemey, S. Hafenstein, and A. M. Lindberg.** 2010. Characterization of a putative  
663 ancestor of coxsackievirus B5. *J. Virol.* **84**:9695-9708. doi: 10.1128/JVI.00071-10 [doi].
- 664 25. **Jonsson, N., A. Savneby, M. Gullberg, K. Evertsson, K. Klingel, and A. M. Lindberg.**  
665 2015. Efficient replication of recombinant Enterovirus B types, carrying different P1 genes in  
666 the coxsackievirus B5 replicative backbone. *Virus Genes.* **50**:351-357. doi: 10.1007/s11262-  
667 015-1177-x [doi].
- 668 26. **Gullberg, M., C. Tolf, N. Jonsson, C. Polacek, J. Precechtelova, M. Badurova, M. Sojka,**  
669 **C. Mohlin, S. Israelsson, K. Johansson, S. Bopegamage, S. Hafenstein, and A. M. Lindberg.**  
670 2010. A single coxsackievirus B2 capsid residue controls cytolysis and apoptosis in  
671 rhabdomyosarcoma cells. *J. Virol.* **84**:5868-5879. doi: 10.1128/JVI.02383-09 [doi].
- 672 27. **Myllynen, M., A. Kazmertsuk, and V. Marjomaki.** 2016. A Novel Open and Infectious  
673 Form of Echovirus 1. *J. Virol.* **90**:6759-6770. doi: 10.1128/JVI.00342-16 [doi].

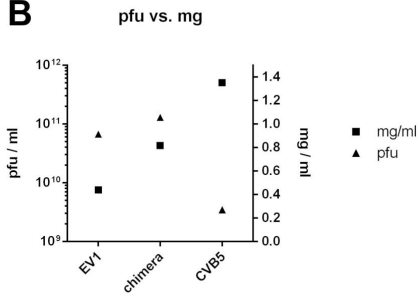
- 674 28. **Carson, S. D., K. S. Kim, S. J. Pirruccello, S. Tracy, and N. M. Chapman.** 2007.  
675 Endogenous low-level expression of the coxsackievirus and adenovirus receptor enables  
676 coxsackievirus B3 infection of RD cells. *J. Gen. Virol.* **88**:3031-3038. doi: 88/11/3031 [pii].
- 677 29. **Chapman, N. M., A. Ragland, J. S. Leser, K. Hofling, S. Willian, B. L. Semler, and S. Tracy.**  
678 2000. A group B coxsackievirus/poliovirus 5' nontranslated region chimera can act as an  
679 attenuated vaccine strain in mice. *J. Virol.* **74**:4047-4056.
- 680 30. **Royston, L., M. Essaidi-Laziosi, F. J. Perez-Rodriguez, I. Piuz, J. Geiser, K. H. Krause, S.**  
681 **Huang, S. Constant, L. Kaiser, D. Garcin, and C. Tapparel.** 2018. Viral chimeras decrypt the  
682 role of enterovirus capsid proteins in viral tropism, acid sensitivity and optimal growth  
683 temperature. *PLoS Pathog.* **14**:e1006962. doi: 10.1371/journal.ppat.1006962 [doi].
- 684 31. **Combelas, N., B. Holmblat, M. L. Joffret, F. Colbere-Garapin, and F. Delpyroux.** 2011.  
685 Recombination between poliovirus and coxsackie A viruses of species C: a model of viral  
686 genetic plasticity and emergence. *Viruses.* **3**:1460-1484. doi: 10.3390/v3081460 [doi].
- 687 32. **Polacek, C., J. O. Ekstrom, A. Lundgren, and A. M. Lindberg.** 2005. Cytolytic replication  
688 of coxsackievirus B2 in CAR-deficient rhabdomyosarcoma cells. *Virus Res.* **113**:107-115. doi:  
689 S0168-1702(05)00157-7 [pii].
- 690 33. **Carson, S. D., N. M. Chapman, S. Hafenstein, and S. Tracy.** 2011. Variations of  
691 coxsackievirus B3 capsid primary structure, ligands, and stability are selected for in a  
692 coxsackievirus and adenovirus receptor-limited environment. *J. Virol.* **85**:3306-3314. doi:  
693 10.1128/JVI.01827-10 [doi].
- 694 34. **Lindberg, A. M., R. L. Crowell, R. Zell, R. Kandolf, and U. Pettersson.** 1992. Mapping of  
695 the RD phenotype of the Nancy strain of coxsackievirus B3. *Virus Res.* **24**:187-196.
- 696 35. **Milstone, A. M., J. Petrella, M. D. Sanchez, M. Mahmud, J. C. Whitbeck, and J. M.**  
697 **Bergelson.** 2005. Interaction with coxsackievirus and adenovirus receptor, but not with  
698 decay-accelerating factor (DAF), induces A-particle formation in a DAF-binding  
699 coxsackievirus B3 isolate. *J. Virol.* **79**:655-660. doi: 79/1/655 [pii].
- 700 36. **Zhang W, Zhang L, Wu Z, and Tien P.** 2014. Differential interferon pathway gene  
701 expression patterns in Rhabdomyosarcoma cells during Enterovirus 71 or Coxsackievirus  
702 A16 infection. *Biochemical and Biophysical Research Communications.* **447**:550-555. doi:  
703 <https://doi.org/10.1016/j.bbrc.2014.04.021>.
- 704 37. **Putnak, J. R., and B. A. Phillips.** 1982. Poliovirus empty capsid morphogenesis: evidence  
705 for conformational differences between self- and extract-assembled empty capsids. *J. Virol.*  
706 **41**:792-800.
- 707 38. **Shingler, K. L., J. L. Yoder, M. S. Carnegie, R. E. Ashley, A. M. Makhov, J. F. Conway, and**  
708 **S. Hafenstein.** 2013. The enterovirus 71 A-particle forms a gateway to allow genome  
709 release: a cryoEM study of picornavirus uncoating. *PLoS Pathog.* **9**:e1003240. doi:  
710 10.1371/journal.ppat.1003240 [doi].

- 711 39. **Basavappa, R., R. Syed, O. Flore, J. P. Icenogle, D. J. Filman, and J. M. Hogle.** 1994. Role  
712 and mechanism of the maturation cleavage of VP0 in poliovirus assembly: structure of the  
713 empty capsid assembly intermediate at 2.9 Å resolution. *Protein Sci.* **3**:1651-1669. doi:  
714 10.1002/pro.5560031005 [doi].
- 715 40. **Cifuentes, J. O., H. Lee, J. D. Yoder, K. L. Shingler, M. S. Carnegie, J. L. Yoder, R. E.**  
716 **Ashley, A. M. Makhov, J. F. Conway, and S. Hafenstein.** 2013. Structures of the procapsid  
717 and mature virion of enterovirus 71 strain 1095. *J. Virol.* **87**:7637-7645. doi:  
718 10.1128/JVI.03519-12 [doi].
- 719 41. **Wang, X., J. Ren, Q. Gao, Z. Hu, Y. Sun, X. Li, D. J. Rowlands, W. Yin, J. Wang, D. I.**  
720 **Stuart, Z. Rao, and E. E. Fry.** 2015. Hepatitis A virus and the origins of picornaviruses.  
721 *Nature.* **517**:85-88. doi: 10.1038/nature13806 [doi].
- 722 42. **Curry, S., E. Fry, W. Blakemore, R. Abu-Ghazaleh, T. Jackson, A. King, S. Lea, J.**  
723 **Newman, and D. Stuart.** 1997. Dissecting the roles of VP0 cleavage and RNA packaging in  
724 picornavirus capsid stabilization: the structure of empty capsids of foot-and-mouth disease  
725 virus. *J. Virol.* **71**:9743-9752.
- 726 43. **Zhu, L., X. Wang, J. Ren, C. Porta, H. Wenham, J. O. Ekstrom, A. Panjwani, N. J.**  
727 **Knowles, A. Kotecha, C. A. Siebert, A. M. Lindberg, E. E. Fry, Z. Rao, T. J. Tuthill, and D. I.**  
728 **Stuart.** 2015. Structure of Ljungan virus provides insight into genome packaging of this  
729 picornavirus. *Nat. Commun.* **6**:8316. doi: 10.1038/ncomms9316 [doi].
- 730 44. **Yuan, T. T., M. H. Lin, D. S. Chen, and C. Shih.** 1998. A defective interference-like  
731 phenomenon of human hepatitis B virus in chronic carriers. *J. Virol.* **72**:578-584.
- 732 45. **Dimmock, N. J., and A. J. Easton.** 2014. Defective interfering influenza virus RNAs: time  
733 to reevaluate their clinical potential as broad-spectrum antivirals? *J. Virol.* **88**:5217-5227.  
734 doi: 10.1128/JVI.03193-13 [doi].
- 735 46. **Li, D., W. B. Lott, K. Lowry, A. Jones, H. M. Thu, and J. Aaskov.** 2011. Defective  
736 interfering viral particles in acute dengue infections. *PLoS One.* **6**:e19447. doi:  
737 10.1371/journal.pone.0019447 [doi].
- 738 47. **Song, Y., A. V. Paul, and E. Wimmer.** 2012. Evolution of poliovirus defective interfering  
739 particles expressing *Gussia luciferase*. *J. Virol.* **86**:1999-2010. doi: 10.1128/JVI.05871-11  
740 [doi].
- 741
- 742

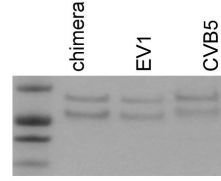
**A**



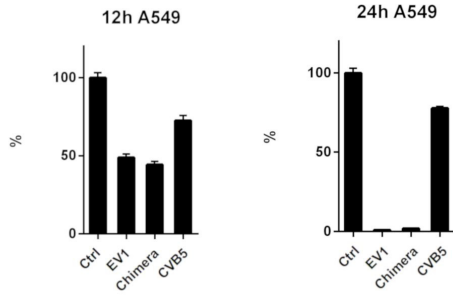
**B**



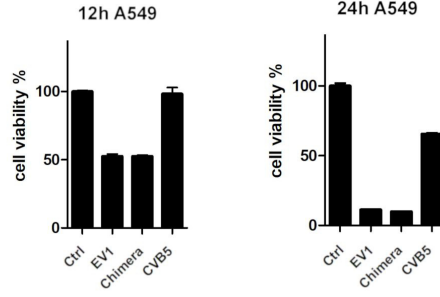
**C**



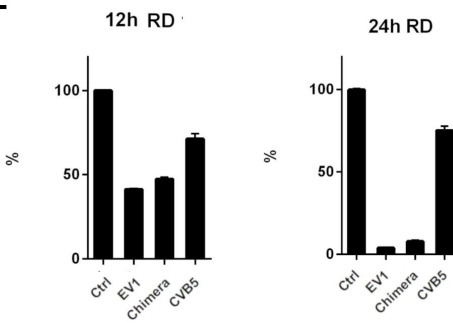
**D**



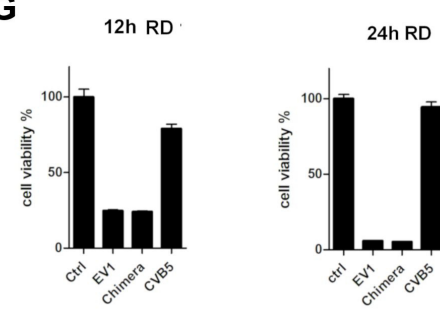
**E**

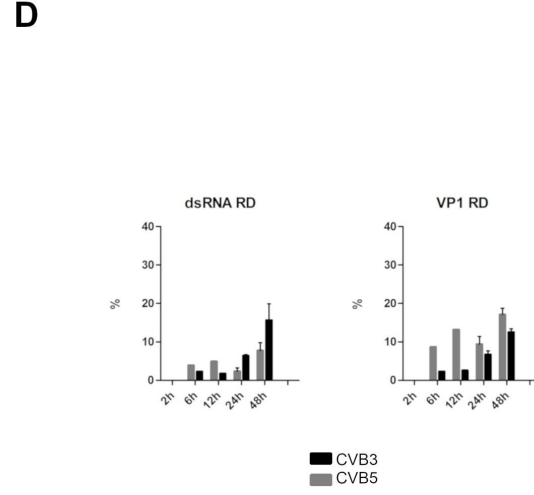
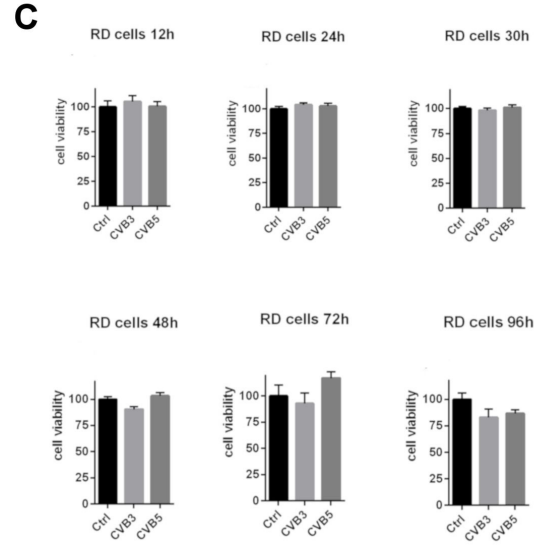
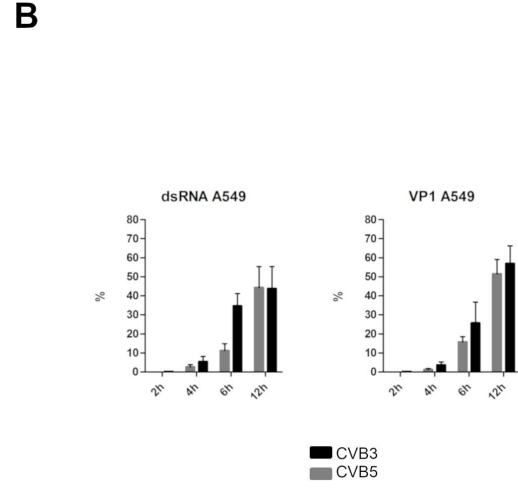
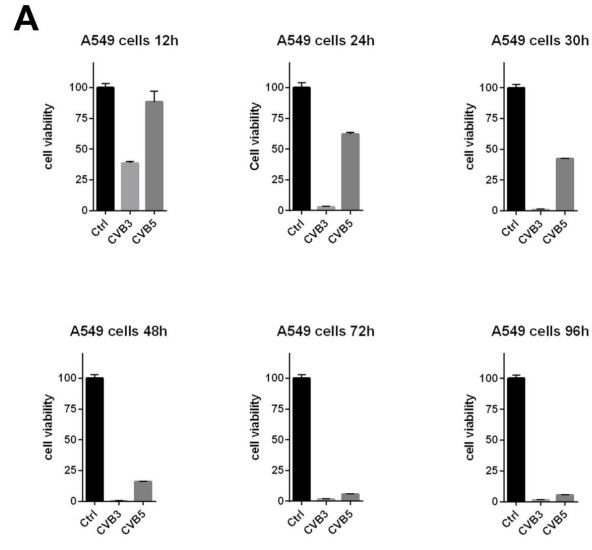


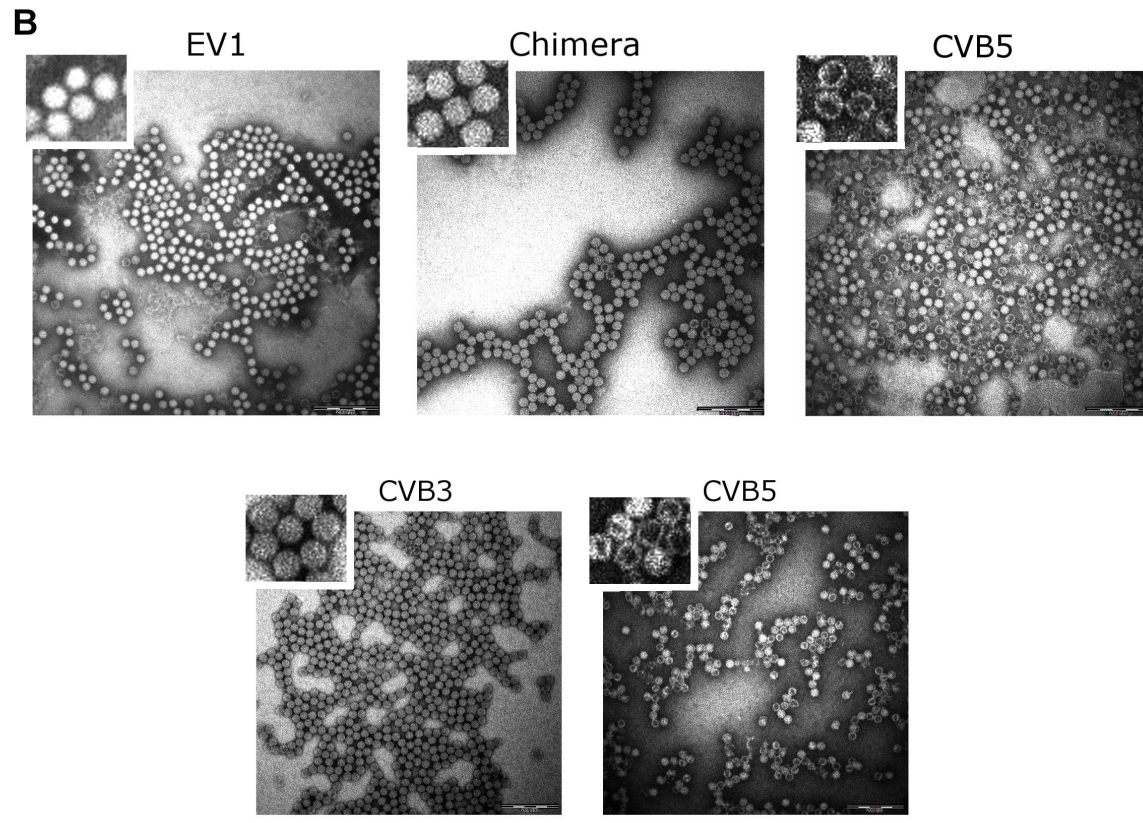
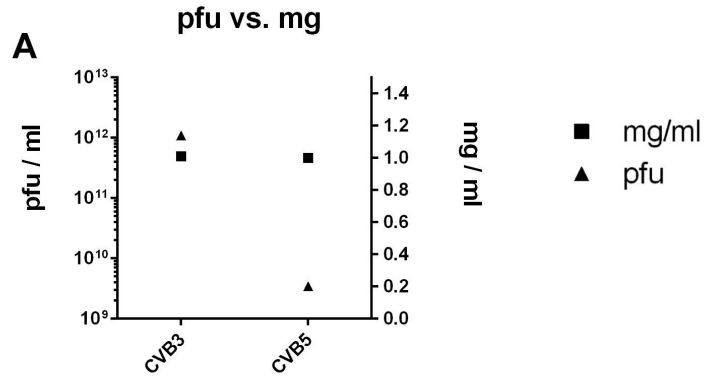
**F**



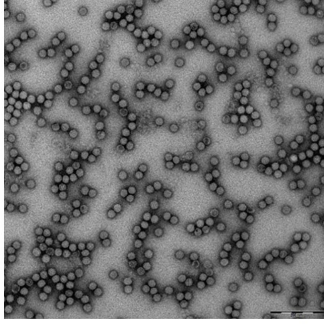
**G**



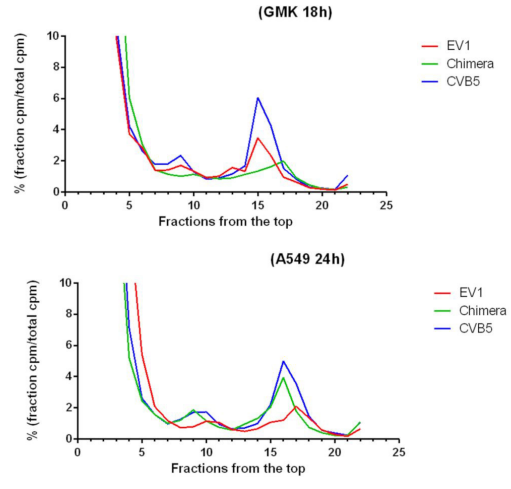




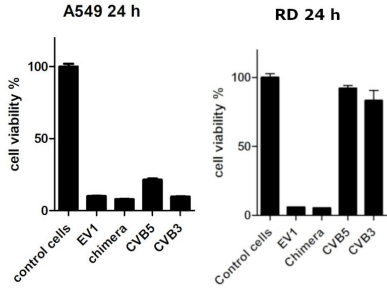
**A**



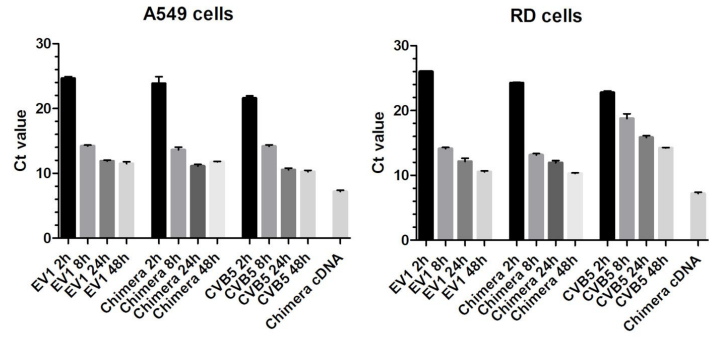
**B**



**C**



**D**



**E**

